Characterization and Dissolution Studies of Salicylic Acid Loaded Multi-Walled Carbon Nanotubes

Mohd Lokman Ibrahim [1, 2, 3*]

[1] School of Chemistry and Environment, Faculty of Applied Sciences, Universiti Teknologi MARA, 40450 Shah Alam, Selangor, Malaysia.
[2]Institute of Science, Universiti Teknologi MARA, 40450 Shah Alam, Selangor, Malaysia.
[3]Industrial Waste Conversion Technology Research, Faculty of Applied Sciences, Universiti Teknologi Mara, 40450 Shah Alam, Selangor
Corresponding author *mohd_lokman@puncakalam.uitm.edu.my

Received: 12 February 2019
Accepted: 11 April 2019
Published: 30 June 2019

ABSTRACT

Multi-walled carbon nanotubes (MWCNTs) have been known as an innovative carrier for drug support and delivery applications. Herein, the modification of MWCNTs was carried out to improve dispersibility and biocompatibility levels. MWCNTs were functionalized by an aqua regia of concentrated nitric acid (HNO_3) and sulfuric acid (H_2SO_4) to produce functionalized MWCNTs (*f*-MWCNTs). Meanwhile, the salicylic acid was loaded on the *f*-MWCNTs by sonication technique and the resultant was coded as *SA*-MWCNTs. Dissolution analysis was carried out in the different medium of simulated body fluid (SBF), simulated gastric fluid (SIF) and simulated gastric fluid (SGF) to evaluate the profile of drug release of *SA*-MWCNTs. It was found that the release profile of aspirin displayed 2-stage of releases; (1) fast release within 1 to 5-hours followed by (2) sustainable release for up to 12-hours. Thus, showing the compatibility of the *f*-MWCNTs for salicylic acid controlled released system.

Keywords: *MWCNTs, Functionalization, Salicylic acid, Adsorption, Dissolution*

INTRODUCTION

Aspirin or also known as acetylsalicylic acid or salicylic acid is one of the most commonly non-steroidal anti-inflammatory drugs (NSAIDs) that have been produced in billions amount yearly. Aspirin is frequently used for the treatment of mild to moderate pain, including migraine and fever [1]. However, due to problems related to administration of free drugs, such as limited solubility, poor biodistribution, lack of selectivity, unfavorable pharmacokinetics and easily damage the healthy tissue give bad side effect in long term. Recently, a drug-CNTs delivery system has been introduced to overcome this problem and it is generally designed to improve the pharmacological and therapeutic profile of a drug molecule [2].

Last decade, quite a number of approaches are emerging in the field of drug delivery, parallel to the significant improvement in advanced nanotechnology such as lipid, peptide or silica nanotubes and carbon nanotubes (CNTs) [2]. The CNTs are tubular carbon materials with a diameter in the nanoscale range. They can be classified by their structure into two main types: (i) single-walled carbon nanotubes (SWCNTs), which consist of a single layer of grapheme sheet seamlessly rolled into a cylindrical tube, and (ii) multi-walled carbon nanotubes (MWCNTs), which comprise of multiple layers of concentric cylinders with a space of about 0.34 nm between the adjacent layers [3]. It also has very interesting physicochemical properties such as ultralight weight [4], high mechanical strength [5], electrical conductivity [6], thermal conductivity [7] and high surface area. All these characteristics build CNTs as one of the unique materials with the potential for diverse application, including molecular electronics [8], supercapacitors [9], biochemical sensor [10] and especially biomedical [11].

According to Sekhar *et al*. [12], a drug with poor solubility could be improved with a good drug delivery system where both hydrophilic and hydrophobic environments exist and thereby would increase the dispersion ability. Besides that, once a drug is released faster and not retained in the infected human body even before the body could assimilate it, the patient needs to use high doses so as to make up for the bioavailability [3, 12]. However, that large dose of the drug may cause damage to the non-infected tissue. Therefore, with a targeted drug delivery system, by altering the pharmacokinetics of the drug, also with regulated drug release can eliminate the said problem. Other than that, poor bio-distribution is also a common problem that can affect normal tissues adversely through unwanted widespread distribution. To overcome, the particulates from the targeted drug delivery system could reduce the rate of distribution and the effect on non-target tissue thereby drastically reducing unwanted side effects [3].

We have included in our work an approach to overcome the poor dispersibility, that is through surface modification of MWCNTs with hydroxyl, carbonyl, and carboxylic groups which were achieved by adsorption, electrostatic interaction or covalently bonded that render them to be hydrophilic. Through such modification, the water solubility of MWCNTs is improved and their biocompatibility profile completely transformed [11]. The true potential of the *f*-MWCNTs as the drug carrier was evaluated by insertion of the drug moieties or a subject drug such as salicylic acid via several chemical processes. The dissolution studies in the simulated fluid mimicking the body condition was carried out to study the trends and profiles of drug release. The data and results were generated from this study proving the ability of the MWCNTs as an example of a drug carrier system and a good reference for further research in the future.

EXPERIMENTAL

Materials

The pristine MWCNTs were purchased from Sun Nanotech Co. Ltd, with a diameter range of 10-30 nm and 90% of purity. The nitric acid, HNO_3 (65%) and sulphuric acid, H_2SO_4 (96%) that used to functionalize MWCNTs were obtained from Merck chemical company. Salicylic acid (SA) used in this work was purchased from Sigma-Aldrich, Inc. Meanwhile, aspirin tablets were purchased from Bayer Corp., consists of 500 mg of SA per tablet (average weight; 600 mg/tablet). The simulated biological fluids such as SBF, SIF, and SGF for the dissolution studies were prepared according to the US standard method of US Pharmacopeia 2000 (USP2000).

Preparation of *f*-MWCNTs

The suspension containing 200 mg of MWCNTs in 350 mL of H_2SO_4:HNO_3 (3:1 / v:v) was ultrasonically vibrated in an ultrasonic bath, model 3510E-DTH, Branson about 40 ºC to 50 ˚C for 2 hrs and let stirred for 24 hrs at ambient temperature. The suspension was added with 250 mL distilled water and separated by centrifugation followed by filtration through a nylon membrane filter (pore size: 0.2 µm). The residues were washed with warm deionized water during filtration until pH 6~7. Finally, the black precipitated *f*-MWCNTs were heated at 80 ºC more than 12 hrs to remove all remaining water.

Preparation of Salicylic Acid-MWCNTs Composite

The salicylic Acid-MWCNTs (*SA*-MWCNTs) composite was prepared by mixing 0.2 g of *f*-MWCNTs into 250 mL of *SA* solution (2%). The suspension was sonicated for 2 hrs and stirred for 24 hrs at ambient temperature. The suspension was then separated from the supernatant by filtration with a nylon membrane filter (pore size: 0.2 µm) and dried at 70 ºC for 12 hrs. The residue was collected and the concentration of the remaining SA was determined using UV-Vis spectrophotometer at a λ=297 nm. The amount of SA loading was calculated according to Eq. 1.

$$[SA]_{\text{loaded}} = [SA]_{\text{initial concentration}} - [SA]_{\text{remaining}} \qquad \text{[Eq. 1]}$$

Characterizations

The Perkin Elmer FTIR spectroscopy model Spectrum One was used to determine the functional groups introduced on the carbon structure after functionalization. The sample of MWCNTs sample was taken approximately 0.5 mg and transferred to a mortar crucible. KBr was added in the ratio of 1:100 (sample: KBr), mixed thoroughly and ground together in the mortar until it becomes a fine homogenous powder. The mixture was then pressed to a pressure to obtain the sample disk. The disk was placed in the sample holder and scanned in the range of 400 to 4000 cm^{-1}.

FE-SEM model JSM-6701F (JEOL) was used to observe the morphological structure of MWCNTs before and after functionalization and also the drug load MWCNTs composite. The MWCNTs has adhered onto carbon tape on a flat surface of an aluminum sample stub, then the micrograph of the sample was taken in the various range of magnification.

A Perkin Elmer UV-vis spectrophotometer, Lambda 25, was used to determine the drug-loaded MWCNTs. Furthermore, the surface area of samples was determined by a classical method based on the concentration of methylene blue adsorbed on the surface of the MWCNTs, which was proportional to the surface area of the MWCNTs [13]. UV absorption for methylene blue was determined at wavelength 670 nm. About 10 mg of sample was added into 10 ppm of methylene blue and was kept for 24 hrs at room temperature. The mixture was then separated by filtration using a nylon membrane filter (pore: 0.2 µm). The absorbance of the supernatant was observed by UV-Vis spectrophotometer and their corresponding concentration was calculated from the calibration curve using Eq. 2.

$$Surface\ area = \frac{Ng\ \times \mathrm{A} \times \mathrm{N} \times 10^{-20}}{M} \qquad (Eq.\ 2)$$

S; Specific surface area,
N_g; Number of methylene blue molecules adsorbed by MWCNTs,
A; Surface area of one methylene blue molecules = 197.2 $Å^2$,
N; Avogadro number = 6.02 x 10^{23} mol^{-1},
M; Molecular weight of methylene blue, 373.9 g mol^{-1}.

The Mettler Toledo thermal gravimetric analyzer (TGA) model TG 50 with the software TC 15 have been used to determine the heat stability and the percentage of the drugs loaded on the surface of MWCNTs. The temperature rate was set at 10 ºC min^{-1} from 50 ºC to 850 ºC. About 6 to 9 mg sample was weighed on a highly sensitive balance over a precisely controlled furnace. Decomposition in the air indicates the processes, which may occur before ignition, while their absence or delay under nitrogen gases is an indication of a condensed phase decomposition mechanism. Mass lost corresponding to the evolution of gases was plotted versus temperature.

Preparation of Simulated Biological Fluids

In this work, three types of simulated biological fluids including simulated body fluid, gastric fluid, and intestinal fluid were prepared mimicking to the real body, gastric and intestinal fluids in the human body. This is very important to analyze the drug release trends in 3 different parts of the human body.

Table 1 shows the reagents and the amount of each chemical needed to prepare 1 L of SBF solution. 750 mL ultrapure water was stirred and heated at 37 ºC in a 1000 mL clean beaker. The chemicals #1 to #8 as given in Table 1 were added carefully. The mixture was stirred until all the chemicals were completely dissolved. Reagent #9 was added slowly (dropwise) to the solution to avoid an increase in the pH of the solution. The pH of the solution was controlled by 0.1 M HCl approximately at pH 7.5 using a pH meter model pH510 (Eutech Instruments) at 37 ºC, 1 M HCl was used to decrease the pH to 7.25. The solution was transferred to a 1.0 L volumetric flask and completed with ultrapure distilled water (double distillation process) and stored with a temperature below than 10 ºC in the fridge [14-17].

Table 1: Reagents to prepare 1 L of SBF (pH 7.24)

Order	Reagent	Note	Amount
#1	NaCl	Assay min. 99.5%, Nacalai tesque, Kyoto, Japan	7.996 g

#2	$NaHCO_3$	Assay (after drying) min. 99.5-100.3%, Nacalai tesque, Kyoto, Japan	0.350 g
#3	KCl	Assay min. 99.5%, Nacalai tesque, Kyoto, Japan	0.224 g
#4	$K_2HPO_4 \cdot 3H_2O$	Assay min. 99.0%, Nacalai tesque, Kyoto, Japan	0.228 g
#5	$MgCl_2 \cdot 6H_2O$	Assay min. 98.0%, Nacalai tesque, Kyoto, Japan	0.305 g
#6	1 kmol m^{-3} HCl	87.28 mL of 35,4% HCl is diluted to 1000 mL with volumetric flask	40 cm^3
#7	$CaCl_2$	Assay min. 95.0%, Nacalai tesque, Kyoto, Japan Use after drying at 120 ^oC for more than 12 hours	0.278 g
#8	Na_2SO_4	Assay min. 99.0%, Nacalai tesque, Kyoto, Japan	0.071 g
#9	$(CH_2OH)_3CNH_2$	Assay (after drying) min. 99.9%, Nacalai tesque, Kyoto, Japan	6.057 g
#10	1 kmol m^{-3} HCl	See above	Appropriate amount for adjusting pH

To prepare 1.0 L of SIF, 650 mL deionized water was stirred and heated at 37 ºC. The 6.8 g monobasic potassium phosphate, KH_2PO_4 was added into the solution and stirred. About 190 mL of 0.1 M NaOH and 10 g of pancreatin were mixed into the solution until totally dissolved. The solution was transferred into a 1.0 L volumetric flask and made up to 1.0 L of SIF solution with ultrapure distilled water. The pH of the solution was determined while the solution temperature is 37 ºC and controlled with 0.1 M NaOH solution until it reached pH 6.6 [18-20]. The composition for SIF is described as in Table 2.

Table 2: Composition of simulated intestinal fluid, pH 6.8, 1 L, USP 26

Composition	mass
KH_2PO_4	6.805 g
0.1 M NaOH	0.896 g
Deionized water	Up to 1 L
Pencreatin	10 g

To prepare 1.0 L SGF, 0.8 L ultrapure water was stirred and heated at 37 ºC. The 2.0 g of sodium chloride, NaCl, 3.2 g of pepsin and 3.0 mL of concentrated HCl was added into the solution. The solution was transferred in a 1.0 L volumetric flask and ultrapure water was added up to the 1.0 L mark. The pH of the solution was verified at pH 1.2-1.5 at a temperature of 37 ºC [21-22].

In Vitro Drug Released Analysis

The dissolution test of drug release study was carried out *in vitro*. The 500 mL beaker was sealed with aluminum foil to keep the temperature constant and to avoid exposure to air. The stirring rate for this test was also kept constant at 100 rpm simulating human churning action in the stomach. Control experiments were done using commercialized drug including aspirin

tablet. SA loading onto the surface of *f*-MWCNTs resulted in 37% of SA contained in the SA-MWCNTs composite. Exactly 20 mg of SA-MWCNTs, equivalent to 6.48 mg SA loaded was used in every test for dissolution analysis in each simulated biological fluid. The parameters used in this work are the temperature and pH of simulated biological fluid.

About 350 mL of SBF solution was heated at 37 ºC and stirred at 100 rpm, followed by addition of 20 mg of SA-MWCNTs in the membrane dialysis tube, transferred into the porous glass tube in the beaker containing SBF solution at 37 ºC. The pH of the solution was recorded every hour using pH meter, while 5 mL of SBF solution was taken every hour up to 24 hrs period for the determination of SA amount. The above method was repeated at 39 ºC and also for the dissolution study of *SA*-MWCNTs in SIF and SGF at 37 ºC and 39 ºC.

RESULTS AND DISCUSSION

Characterization analysis

FTIR was used to analyze the changes on the surface species of nanotubes, in the wavenumber range of 400 to 4000 cm^{-1}. The treatment of MWCNTs with the concentrated H_2SO_4 and HNO_3 introduced several functional groups on the structure including carboxylic, carbonyl, and hydroxyl groups. Interpreting FTIR spectra for these compounds were complicated as the frequency ranges for the different classes of carbonyl (C=O) compounds overlap. The carbonyl group also will affect the frequencies of other additional functionalities (like C–O, C–N, and N–H) because it is an electron withdrawing group. Hence, observed wavenumber will be different than the one reported in the literature [23-24].

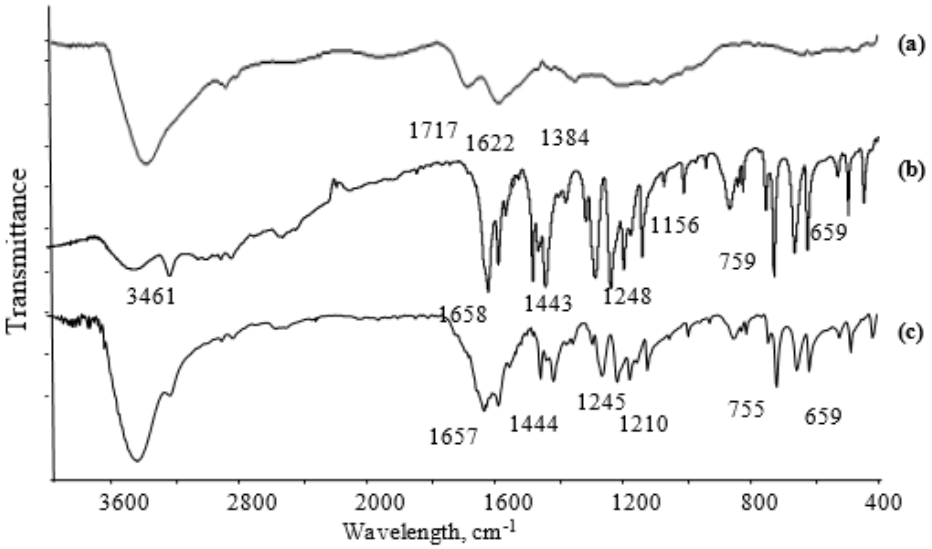

Figure 1: IR spectra of (a) MWCNTs (b) Salicylic acid and (c) *SA*-MWCNTs

Figure 1 shows the IR spectra of MWCNTs of (a) *f*-MWCNTs, (b) aspirin and (c) SA-MWCNTs. The spectra, which depicted broad absorption band in the range of 3430 - 3400 cm^{-1} that is assigned for hydroxyl (-OH) functionality due to the water present within the samples and the carboxylic group introduced on the structure. Figure 1(a); the absorption peaks around 1622 cm^{-1} and 1384 cm^{-1} clearly show the presence of a carbon double bond (C=C) sp^2 bonding with the aromatic double bond of the carbon structure. The absorption band which appeared

after the oxidation at 1717 cm^{-1} due to the generated carbonyl (C=O) sp^2 bonding, which is lower than the theoretical peaks because C=O is adjacent to the O-H withdrawing group [25-26]. This latter mode, together with the mode around 1540 cm^{-1} (not shown), resembles the characteristic modes of graphite at 868 and 1590 cm^{-1} [27]. From this spectra, it clearly indicates the oxidation of MWCNTs surface and the presence of –COOH groups on the structure.

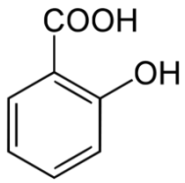

Figure 2: Molecular structure of acetylsalicylic acid

Figure 2 shows the molecular structure of the salicylic acid molecule. It can be observed that most of the IR absorptions detected in the spectrum of SA in Figure 1(b) are present in the spectrum of SA-MWCNTs in Figure 1(c). The functional groups presented on both samples are a carboxylic group (-COOH), carbonyl (C=O), and hydroxyl (-OH) groups. These functional groups assigned at absorption 1658 cm^{-1} (Figure 1b) and 1657 cm^{-1} (Figure1c) for C=O, and the broadband detected in the range of 3200-3400 cm^{-1} is for O-H groups. We can conclude that the IR absorptions for SA were detected in the spectrum SA-MWCNTs. The SA was successfully loaded and interacted by covalent bonding onto the structure of *f*-MWCNTs.

FESEM analysis was used to investigate the morphological changes of the CNTs, before and after functionalization. Figure 3a and 3b show the micrographs of pristine MWCNTs and *f*-MWCNTs, respectively. From the qualitative point of view, all samples showed diameter in the range of 20-50 nm for the multi-walled tube, compared to the theoretical diameter for single-walled carbon nanotubes (SWCNTs) which is about 0.2 to 2 nm [28].

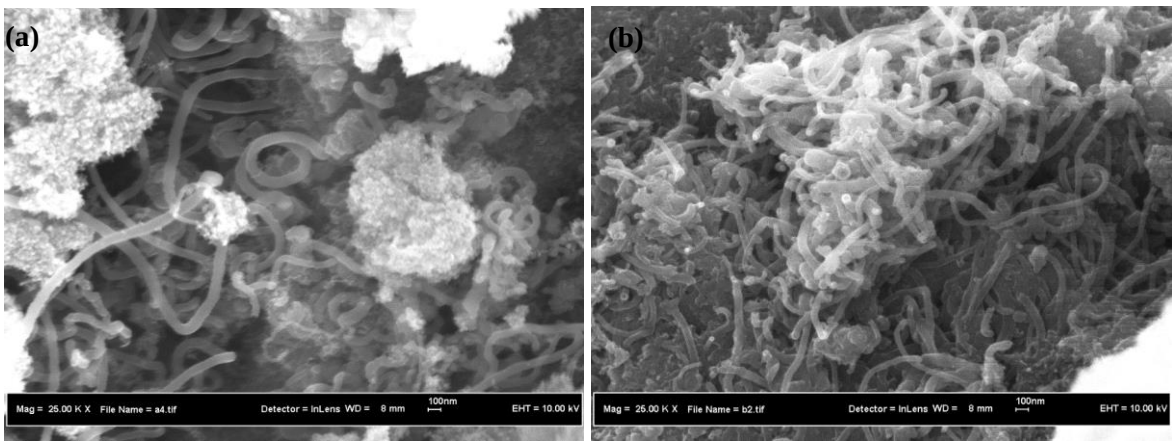

Figure 3: FESEM micrographs of (a) MWCNTs and (b) *f*-MWCNTs (magnification x 25,000)

Several significant changes of the structure after functionalization via both sonication was also observed in Figure 3; the smooth surface of the MWCNTs was transformed to a shorter, rough and groovy surface. The rough and groovy surface of the sidewalls of acid-treated MWCNTs was possibly associated to the defect that occurred due to some slight structure damage, as reported by Kumar *et al.* [26] and Lee *et al.*, 2008 [25]. It also showed some of the *f*-MWCNTs tips were exposed after the treatment with H_2SO_4:HNO_3 (3:1) via

sonication, indicated the breaking of the carbon-carbon bond along with the graphene of nanotubes, thus, allowing the formation of functional groups on the open end of the carbon tubes [29].

In this work, the surface area of *f*-MWCNTs was determined using the classical method to measure the adsorption of methylene blue onto the surface of *f*-MWCNTs. The amount of the methylene blue adsorbed on the structure of MWCNTs is directly proportional to the surface area of the CNTs, and it was calculated according to the Eq. 2.

Table 3 shows the surface area of MWCNTs and *f*-MWCNTs. From this test, it was found that the surface area of raw MWCNTs was 283.2 m^2g^{-1}, has been reported in previous literature, the average surface area of raw MWCNTs is in the range of 50 to 1315 m^2g^{-1} [30]. Meanwhile, the surface area of *f*-MWCNTs was 535.8 m^2g^{-1} after functionalization process, this may be due to the defect and the reduction of tube-length of the MWCNTs. According to Son *et al*. [31] and Lee *et al*. [25], the short length of the nanotube will provide more sites for the anchoring of drug molecules because of the high surface area.

Table 3: Surface area of MWCNTs

Samples	Surface area ($m^2 g^{-1}$)
MWCNTs	283.2 ± 3.0
f-MWCNTs	535.8 ± 8.8

According to Foldvari and Bagonluri [32], it is essential that MWCNTs must be dispersed before they are used in therapeutic formulations and the biocompatibility will increase when increases the water dispersibility through chemical modification of MWCNTs. Hence, this will give advantage for the drug to be transported to the affected sites.

Figure 4 shows the dispersion behavior of SA-MWCNTs in water, SBF, SIF, and SGF at 0h up to 5 days. The presence of functional groups such carboxylic acid, carbonyl and hydroxyl groups on the structure of *f*-MWCNTs resulted from a stable suspension in the solution medium due to the different charge and polarity of the solution, hence it had increased the dispersibility properties of the drug composite. The images also showed that *f*-MWCNTs seem to be more dispersed in water and SIF compared to SBF and SGF, which can also be explained by the functional groups and the charges of SA which gave more hydrophilic effect in the water and SIF compared to SBF and SGF. Basically, this phenomenon gave a positive effect on the drug composite as it helps in the delivering and adsorption of the active drug ingredient by the vilus.

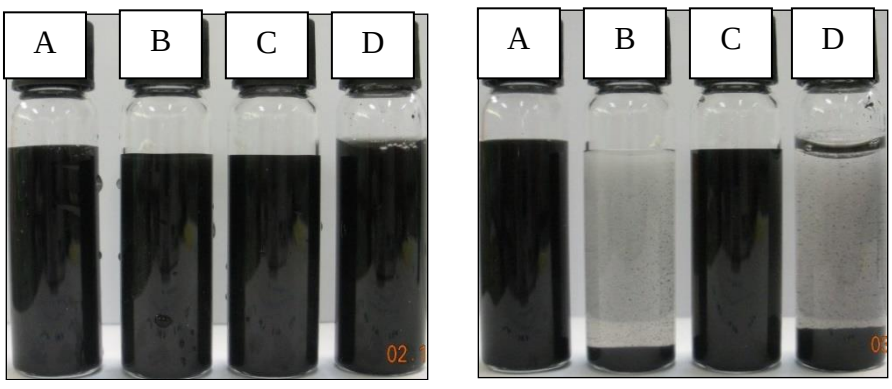

0 hour 2 hours

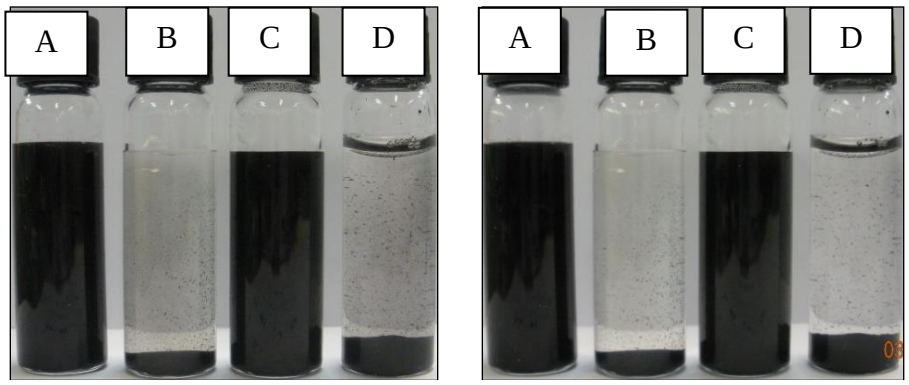

Figure 4: Dispersion behavior of SA-MWCNTs in (A) water, (B) SBF, (C) SIF and (D) SGF

Thermal analysis is a measurement of a change in properties as the temperature changes or elevated, which can be used for the quantitative and qualitative study by identifying the thermal stability of the structure. Figure 5 shows the derivative thermogravimetry (DTG)-TGA of *f*-MWCNTs and *SA*-MWCNTs in nitrogen gas at a heating rate of 10 ºC min^{-1}, within the temperature range of 50 to 850 ºC. The thermograms showed the decomposition stage in the range temperature of 350 to 550 ºC for the *SA*-MWCNTs. The percentage of decomposition at a certain stage can be calculated from DTG thermogram that showing the percentage of the SA on the structure of the nanotubes.

The percentage of drugs loaded was calculated from the percentage of weight loss from the initial weight of the samples. The figure showed a slight decrease in T_{max} of the thermograms for *SA*-MWCNTs, due to the presence of SA molecules (~20 wt.%) which start decomposed at a temperature over than 80 ºC. In addition, the thermogram of *f*-MWCNTs also showing the temperature that needed to combust the carbon tube is very high (>600 ºC), since it is inert and very stable due to the carbon-carbon sp^2 bonding - strengthened the graphene structure of MWCNTs.

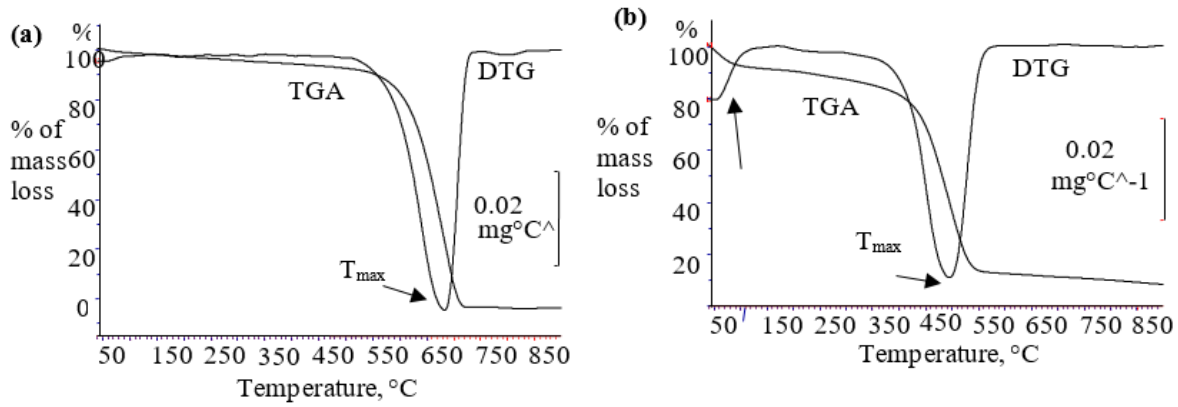

Figure 5: TG-DTG thermograms of (a) *f*-MWCNTs and (b) *SA*-MWCNTs

Adsorption Study of *SA*-MWCNTs

In order to determine the amount of drug loaded onto *f*-MWCNTs, a UV-Vis spectrophotometer (model Lambda 25, Perkin Elmer) was used for quantitative detection of SA molecule. The effects of drug concentration, contact time and degree of functionalization on the drug loading have been studied by Siti Hajar Alias [33] who reported that there were no significant differences in the amount of drug loaded onto the *f*-MWCNTs at different drugs concentration and contact time as long as the same amount of *f*-MWCNTs was used. In this work, it was observed that the adsorption of SA onto *f*-MWCNTs was higher (38.8%) then *non-f*-MWCNTs (20%) as shown in Figure 6. This is due to the functional groups generated on the surface provide sites for anchoring drug molecules.

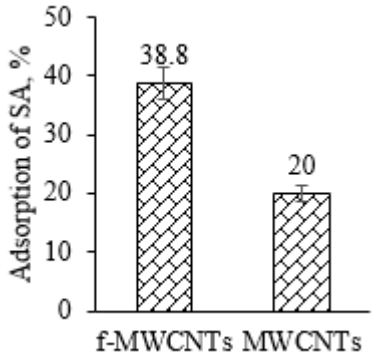

Figure 6: The adsorption capacity of the SA molecules on the *f*-MWCNTs and raw MWCNTs

In Vitro Drug Release Analysis

In this work, several parameters which potentially affect the release rate of drug molecules were studied; such as temperature and type of medium, contact time and pH. According to Sang *et al.* [34], Singh and Kim [35] and Das *et al.* [36], the release rate of the drug molecules is dependent on a few factors such as hydrogen bonding, the solubility, and size of the carrier. Furthermore, different in a chemical group and the pH of the solution also alter the strength of the interaction - the stronger the interaction between *f*-MWCNTs and drug molecules the slower the release rate of the drug molecules will be.

Effect of medium's temperature on the release rate

The release rate of SA from *SA*-MWCNTs in SBF, SIF and SGF at 37 °C and 39 ºC, respectively represent the healthy and non-healthy body temperature were depicted in Figure 7. Despite an identical trend of drug released at 37 ºC and 39 ºC, the figure showed a higher release rate for the first 5 hrs (1st stage) at 0.233 mg/h, 0.402 mg/h and 0.246 mg/h in SBF, SIF and SGF, respectively. Followed by the sustainable release of SA up to 24th hrs at 0.218 mg/h, 0.428 mg/h, and 0.285 mg/h in SBF, SIF and SGF, respectively. The fast release of the drug in the first stage was possibly due to the stacking of drug molecules on the structure. While the strongly bound SA with the surface of *f*-MWCNTs exhibited sustainable release after 5 hrs of the dissolution test.

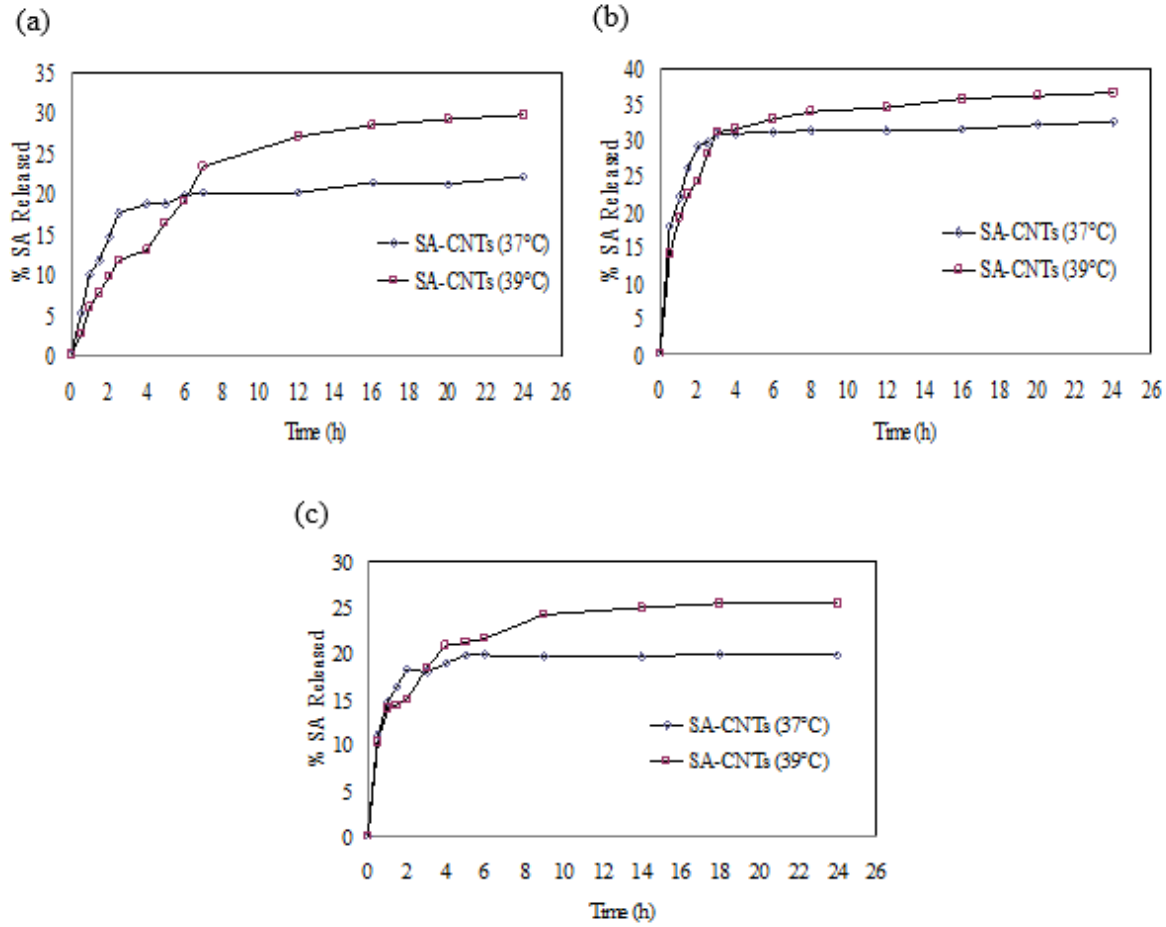

Figure 7: SA release profile of *SA*-MWCNTs in a simulated biological fluid (a) in SBF, (b) in SIF and (c) in SGF at 37 ºC and 39 ºC

A similar observation was reported by Xu *et al.* [37], on the slow release of vancomycin hydrochloride drugs after a few hours from single-walled carbon nanohorn, which occurs due to the stacking of the aromatic rings which are strongly bound to the surface of carbon nanohorns. On the other hand, some attached and trapped drugs do not have strong interaction with the carrier, causing the initial quick release of the drugs [38]. From these observations, the composite could be used for fast and slow drug release, especially when it is required in other parts of the gastrointestinal, GI tract. This is important when one considers hypertensive individuals and the amount of medicine that they ingest. In a system of slow release, individuals

could reduce the amount of ingested drugs, reducing the stress factor and improving their quality of life [39].

Comparison of release rate performances of SA-MWCNTs and commercialized aspirin

In order to evaluate the performance of SA-MWCNTs composite, a controlled study was carried out using commercialized aspirin which consists of 83.3% of SA. Figure 8 shows the SA release profile from *SA*-MWCNTs and aspirin tablet in different simulated biological fluids. *SA*-MWCNTs which was prepared by a 3:1 mixture of H_2SO_4:HNO_3, showed almost 20% of the SA was released within the first 5hrs in SBF, meanwhile in SIF showed almost 30% of the SA was released, followed by a sustained release at 25 - 30% within 24 hrs. Furthermore, the trends also showed 10 - 15% of SA was released from commercialized aspirin within 5 hrs in all SBF, SGF, and SIF followed by increasing and sustained release of SA between 25 - 30% within 24 hrs. However, it is lower than the rate of SA released from *SA*-MWCNTs for the first 5 hrs might be due to the strong attachment of the SA with the polymer and binder in the tablets of aspirin.

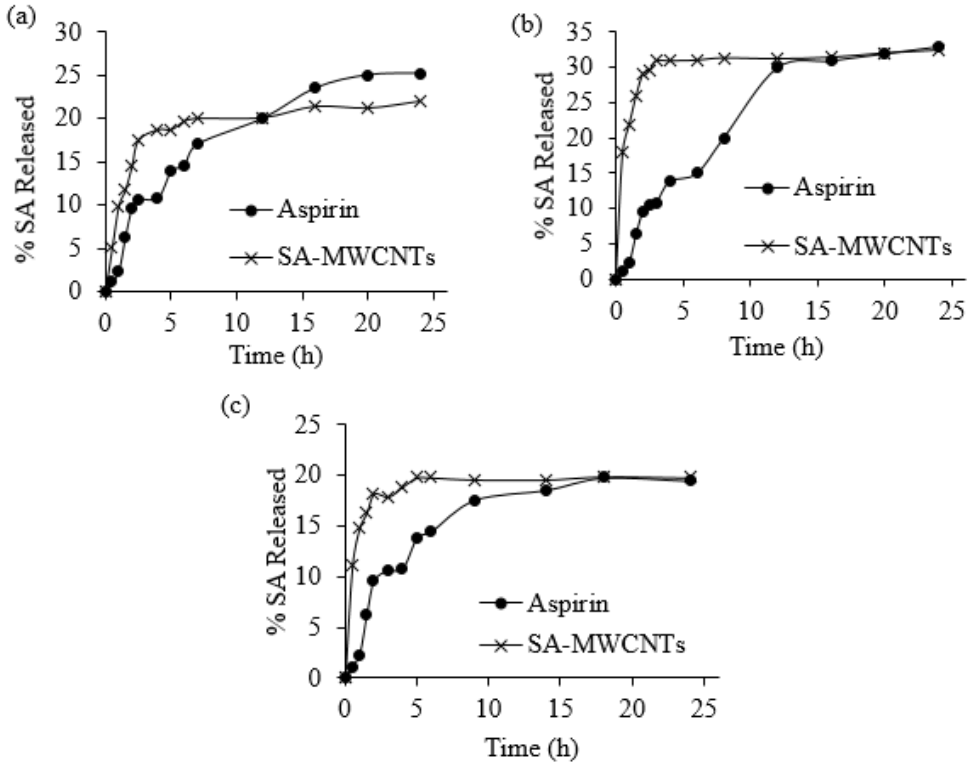

Figure 8: SA release of *SA*-MWCNTs and Aspirin tablet in (a) SBF, (b) SIF and (c) SGF

CONCLUSIONS

The functionalization of MWCNTs was successfully carried out. The FESEM micrographs, TGA thermogram, IR spectra, surface area analysis, and dispersion behavior test had proven the functionalization via aqua regia of concentrated acid 3:1 (H_2SO_4:HNO_3 / v:v) by sonication technique generated high amount of functional groups such as carboxylic acid, carbonyl, and

hydroxyl groups and also creates high surface area which provides more sites for anchoring the SA molecules.

Drug loading analysis showed SA successfully incorporated on the surface of *f*-MWCNTs with lesser than the amount of active ingredient in the commercialized aspirin tablet thus could avoid from the overdose of the drug consumed, without reducing the drug efficiency of *SA*-MWCNTs complexes. While, the dissolution study of SA showed the release of active ingredient was divided into two stages; firstly, the first 5 hrs of fast release, followed by the second stage of sustainable release. This trend gave an advantage to the patient or consumer during the current clinical therapy, patients after treatment within a short time are still mainly treated after a long time by repetitive drug administration release.

Thus, this controlled-release drug delivery systems have been thought to be necessary to improve therapy. The performances and efficiencies of the drug-MWCNTs studied in this work are comparable with the commercialized drugs available. As a summary, this report showing the *f*-MWCNTs could be used in the pharmaceutical industry as novel biomaterials composite with high potential application in drug delivery, dental and orthopedic materials, thus offering the potential exploitation of CNTs as the drug delivery systems, and of course, the next clinical test must be completed prior for the commercialization.

ACKNOWLEDGMENT

The author would like to thank Universiti Teknologi Malaysia, Skudai Johor for the facilities and chemicals supplied throughout the experimentation and analyses. Financial assistance from the 600-IRMI/MyRA 5/3/LESTARI (054/2017) and 600-IRMI/PERDANA 5/3 BESTARI (088/2018) provided by Universiti Teknologi MARA, Shah Alam Selangor are appreciated.

REFERENCES

[1] Benamouzig R., Low-Dose Aspirin and Small Bowel Enteropathy: Mountain or Molehill?, *Digestion* 79:40-41 (2009).

[2] Bianco A., Kostarelos K., Partidos C.D., Prato M., Biomedical applications of functionalised carbon nanotubes, *Chem. Commun*., 571-577 (2005).

[3] Prato M., Kostarelos K., Bianco M., Functionalized carbon nanotubes in drug design and discovery, *Acc. Chem. Res*. 41(1):60-68 (2008).

[4] Chen T., Wang S., Yang Z., Feng Q., Sun X., Li L., Wang Z.S., Peng H., Improving the mechanical properties of carbon nanotubes reinforced pure aluminum matrix composites by achieving non-equilibrium interface *Angewandte Chemie* – Inter. Ed. 50:1815-1819 (2011).

[5] F.L. Jia, J.M. Gong, K.W. Wong, R.X. Simple co-electrodeposition of functionalized multi-walled carbon nanotubes/chitosan composite coating on mainspring for enhanced modulus of elasticity *Nanotech* 20:015701(2009)

[6] Kiamahalleh M.V., Sata S.A., Buniran S., Zein S.H.S., Remarkable stability of supercapacitor material synthesized by manganese oxide filled in multiwalled carbon nanotubes. *Curr. Nanosci.* 6:553-559 (2010).

[7] Berber S., Kwon Y.K., Tomanek D., Unusually High Thermal Conductivity of Carbon Nanotubes. *Phy. Rev. Lett*., 84:4613-4616 (2000).

[8] Avouris P., Molecular Electronics with Carbon Nanotubes Acc. Chem. Res. 35:1026-1034 (2002).

[9] Kiamahalleh M.V., Cheng C.I., Sata S.A., Buniran S., Zein S.H.S., Future scope and directions of nanotechnology in creating next-generation supercapacitors *Nano* 5:143-148 (2010).

[10] El-Ansary A., Faddah L.M., Nanoparticles as biochemical sensors *Nanotechnol. Sci. Appl*. 3:65-76 (2010).

[11] Lacerda L., Bianco A., Prato M., Kostarelos K., Carbon nanotubes as nanomedicines: from toxicology to pharmacology *Adv. Drug Deliv. Rev.* 58:1460-1470(2006).

[12] Jong W.H.D., Borm P.J.A., Drug delivery and nanoparticles: Applications and hazards, Int J Nanomedicine 3(2):133-149 (2008).

[13] Kaewprasit C., Hequet E., Abidi N., Gourlot J.P., Quality Measurement: Application of Mehtylene Blue Adsorption to Cotton Fiber Specific Surface Area Measurement: Part I. *J. Cotton. Sci*. 2:164-173(1998).

[14] Li P., Ohtsuki C., Kokubo T., Nakanishi K., Soga N., Nakamura T., Yamamuro T., Process of formation of bone-like apatite layer on silica gel *J. Mater. Sci. Mater. Med*. 4:127-131 (1993).

[15] Lu X., Leng Y., Theoritical analysis of calcium phosphate precipitation in simulated body fluid *Biomaterials*. 26:1097-1108(2005).

[16] Xin F., Jian C., Jian-Peng Z., Qian W., Zhong-Cheng Z., Jian-Ming R., Bone-like apatite formation on HA/316L stainless steel composite surface in simulated body fluid *Trans*. *Nonferrous. Met. Soc. China*, 19:347-352(2009).

[17] Van der Wal E., Wolke J.G.C., Jansen J.A., Vredenberg A.M., Initial reactivity of rf magnetron sputtered calcium phosphate thin films in simulated body fluids *Appl. Surf. Sci*. 246:183-192(2005).

[18] Stippler E., Kopp S., Dressman J.B., Comparison of US Pharmacopiea Simulated Intestinal Fluid TS (without pancreation) and Phosphate Standard Buffer pH 6.8, TS of the International Pharmacopiea with Respect to Their Use in *In Vitro* Dissolution Testing. *Dissolut. Technol*. 11:6-10 (2004).

[19] Ingels F., Beck B., Oth M., Augustijins P., Effect of simulated intestinal fluid on drug permeability estimation across Caco-2 monolayers *Int. J. Pharm*. 274:221-232(2004).

[20] Fatouros D.G., Walrand I., Bergenstahl B., Mullertz A., Physichochemical Characterization of Simulated Intestinal Fed-Phosphatidylcholine and Cholesterol *Dissolut. Technol*. 7:47-50 (2009).

[21] Herman R.A., Korjagin V.A., Schafer B.W., Quantitative measurement of protein digestion in simulated gastric fluid. *Regul. Toxicol. Pharm*. 41:175-184 (2005).

[22] Yuk H.G., Schneider K.R., Adaption of *Salmonella* spp. in juice stored under refrigerated and room temperature enhances acid resistance to simulated gastric fluid. *Food Microbiol.* 23:694-700 (2006).

[23] Singh R., Pantarotto D., Lacerda L., Pastorin G., Klumpp C., Prato M., Bianco A., Kostarelos K., Tissue biodistribution and blood clearance rates of intravenously administered carbon nanotube radiotracers *Proc Natl Acad Sci USA* 103:3357-3362 (2006).

[24] Dibyendu S.B., Rama D., Zhang N., Xie J., Varadan D.L., Mathur G.N., Chemical Functionalization of Carbon Nanotubes with 3-methacryloxypropyltrimethoxysilane (3-MPTS). *Smart Mater. Struct*. 13:1263-1267 (2004).

[25] Lee G.W., Kim J., Yoon J., Bae J.S., Shin B.C., Kim I.S., Oh W., Ree W., Structural characterization of carboxylated multi-walled carbon nanotubes. *Thin Solid Films*. 516 5781-5784 (2008).

[26] Kumar N.J., Ganapathy H.S., Kim J.S., Jeong S.J., Jeong T.J., Preparation of Poly 2-Hydroxyethyl Methacrylate Functionalized Carbon Nanotubes as Novel Biomaterial Nanocomposites. *Eur. Polym. J.* 44:579-586 (2008).

[27] Branca C., Frusteri F., Magazu V., Characterization of Carbon Nanotubes by TEM and Infrared Spectroscopy. *J. Phys. Chem. B*, 108:3469-3473(2004).

[28] Loos J., Grossiord N., Koning C.E., On the fate of carbon nanotubes: morphological characterizations. *Regev, Comp. Sci. Technol*. 67:783-788 (2007).

[29] Kathi J., Rhee K.Y., Lee J. H., Effect of Chemical Functionalization of Multi-Walled Carbon Nanotubes with 3-Aminopropyltriethoxysilane on Mechanical and Morphological Properties of Epoxy Nanocomposites. *Composites: Part A.* 40:800-809 (2009).

[30] Peigney A., Laurent C., Flahaut E., Bacsa R.R., Rousset A., Specific Surface Area of Carbon Nanotubes and Bundles of Carbon Nanotubes. *Carbon*. 39:507–514 (2001).

[31] Son S.J., Bai X., Lee S.L., Inorganic hollo nanoparticles and nanotubes in nanomedicine, Part 1. Drug/gene delivery applications. *Drug Disc. Today*. 12:650-656 (2007).

[32] Foldvari M., Bagonluri M., Carbon nanotubes as functional excipients for nanomedicines: I. pharmaceutical properties *Nanomed. Nanotechnol. Bio. Med.* 4:173-182 (2008a).

[33] Siti Hajar Alias. “Functionalization of Multi-walled carbon nanotube for aspirin drug delivery system”. Faculty of science, UTM (2009).

[34] Sang J.S., Xia B., Anjan N., Hamidreza G., Sang B.L., Complete Synthesis of Multifunctional Nanotubes for Controlled Release. *J. Control Release*, 114:143-152 (2006).

[35] Singh B.N., Kim K.H., Floating drug delivery systems: an approach to oral controlled drug delivery via gastric retention *J. Control Release,* 63:235-259 (2000).

[36] Das S.K., Kapoor S., Yamada H., Bhattacharyya A.J., Effects of surface acidity and pore size of mesoporous alumina on degree of loading and controlled release of ibuprofen. *Micropor. Mesopor. Mat*. 118:267-272 (2008).

[37] Xu J., Yudasaka M., Kouraba S., Sekido M., Yamamoto Y., Iijima S., Single wall carbon nanohorn as drug carrier for controlled release. *Chem. Phys. Lett.* 461:180-192 (2008).

[38] Rashid R.A., Ishak M.A.M., Hello K.M., Adsorptive removal of methylene blue by commercial coconut shell activated carbon. *Sci Lett*. 12:77-101 (2018).

[39] Ribeiro C., Arizaga G.G.C., Wypych F., Sierakowski M.R., Nanocomposites coated with xyloglucan for drug delivery: *Int. J. Pharm*. 367:204-210 (2009).